Wheat responds to lack of root hairs with recruitment of bacteria harboring P mineralization genes and increased arbuscular mycorrhizal colonization

Courtney Horn Herms[1], Ian Tsang[2,3], Frederik Bak[1], Klara Gunnarsen[1], Magdalena Hasenzagl[1], Amaru Miranda Djurhuus[1], Tom Thirkell[4], Eric Ober[2], Fiona Leigh[2], James Cockram[2], Mette Haubjerg Nicolaisen[1]

1) Department of Plant and Environmental Sciences, University of Copenhagen, Thorvaldsensvej 40, 1871 Frederiksberg, Denmark

2) Niab, Park Farm, Histon, Cambridge, CB24 9NZ, United Kingdom

3) School of Biosciences, University of Nottingham, Sutton Bonington, Loughborough LE12 5RD, United Kingdom

4) Department of Plant Sciences, University of Cambridge, Cambridge, CB3 0LE, United Kingdom

Corresponding Author: Mette Haubjerg Nicolaisen; email: meni@plen.ku.dk

ORCIDs: C.H.H.: 0000-0002-7363-3189; I.T.: 0009-0006-1999-3251; F.B.: 0000-0001-9580-8018; K.G.: 0000-0001-8176-8844; M.H.: no ORCID; A.M.D.: 0000-0003-3762-2922; T.T.: 0000-0002-4481-0924; E.O.: 0000-0002-4832-5897; F.L.: 0000-0002-3221-5327; J.C.: 0000-0002-1014-6463; M.H.N.: 0000-0002-0983-2466

Summary

- Plant roots simultaneously rely on root hairs and the rhizosphere microbiome to acquire phosphorus (P) from the soil, but the full potential of the plant to utilize its microbiome for nutrient capture has yet to be fully understood. We hypothesized that a wheat mutant defective in root hair elongation would recruit more P-cycling bacteria and AMF compared to its wild-type background to compensate for the loss of root hairs.
- Through quantitative polymerase chain reaction and staining, we quantified the enrichment of bacterial P-cycling genes and arbuscular mycorrhizal fungi (AMF) colonization across different stages of wheat development and in differentially P fertilized soils in the presence and absence of root hair elongation.
- The loss of root hair elongation led to an enrichment of P-cycling bacteria during early seedling development, and P mineralizing bacteria dominated over P solubilizing

bacteria. The AMF symbiosis was only fully established after several weeks of growth, and the loss of root hair elongation promoted mycorrhizal formation.

- Wheat can recruit and utilize bacterial P mineralization to meet its P needs before the AMF symbiosis is established, but the colonization of these bacteria is no longer prioritized once the AMF symbiosis is developed.

Key Words

Arbuscular mycorrhizal fungi (AMF), phosphorus (P) cycling, plant-microbe interactions, rhizosphere microbiome, root hairs, *Triticum aestivum* (wheat)

Introduction

Agricultural productivity is often constrained by nutrient availability. Phosphorus (P) is an essential nutrient and vital for central biochemical processes in the plant (Rengel et al., 2022). However, despite a relatively large amount of total P in many soils, bioavailable P is limited in the soil environment, restricting plant growth and yield (Menezes-Blackburn et al., 2018). Thus, P is one of the most heavily applied nutrients to agricultural fields, but P fertilizer is poorly absorbed by the plant (Simpson et al., 2011), leading to runoff into the environment and eutrophication (Ulén et al., 2007). Furthermore, raw phosphate rock used to make P fertilizer is a finite resource with high energy demands for production (Van Kauwenbergh, 2010), further impacting the sustainability of current P fertilization practices. As the need to grow more food using reduced inputs becomes critical to future food security, research is increasingly focusing on ways to improve crop P nutrition under reduced chemical inputs.

Recently, belowground plant traits have become a focus for the improvement of plant nutrition under low fertilizer input (Ober et al., 2021). For example, root hairs elongate under low-P conditions and help the plant access greater volumes of soil, improving access to nutrients (Bates & Lynch, 1996; Tsang, Atkinson, et al., 2024). However, increasing root hair length has a maximum capacity to improve plant P uptake, and further augmentation may lead to negative pleotropic effects such as reduced aboveground biomass (Brown et al., 2012; Zhang et al., 2018). Other mechanisms for plant nutrition that complement root function and performance will therefore need to be integrated into future crops.

Improving beneficial interactions between the plant and its microbiota is another promising target for sustainable plant nutrient uptake (Ge & Wang, 2025). The microbiome in the rhizosphere, the soil volume influenced by plant roots, provides many vital functions for crop health, including P acquisition. Symbiotic arbuscular mycorrhizal fungi (AMF) are especially important for plant P uptake (Smith & Smith, 2011), including in globally important crops such as wheat (*Triticum aestivum* L.) (Thirkell et al., 2020, 2022). When lacking P, plants can selectively boost colonization by AMF to increase their P uptake (Kumar et al., 2019; Zhou et al., 2022). The bacterial fraction of the rhizosphere microbiome also carries functions relating to the cycling of both organic and inorganic P (Bergkemper et al., 2016). Single bacterial isolates demonstrate the ability to increase crop P nutrition and have been suggested as promising bio-based fertilizers (Azaroual et al., 2020; Jensen et al., 2024). However, compared to AMF, much less is known about the ability of the plant to actively enrich and utilize bacterial communities to increase P nutrition.

Unraveling how plants enrich both AMF and bacteria to improve P nutrition may inform strategies to leverage plant-microbe interactions under reduced agricultural inputs. However,

it has not yet been shown that crops can enrich bacteria with P-cycling abilities in the rhizosphere under P-deficient conditions, potentially due to the dominance of other mechanisms for increasing P uptake, namely elongation of root hairs (Bates & Lynch, 1996). In this work, we used the recently developed wheat root hair mutant *short root hair 1* (*srh1*) (Tsang, Thomelin, et al., 2024) to assess the ability of wheat to leverage the soil microbiome for P nutrition when root hair elongation is absent, which is the dominant plant response to P limitation that can otherwise obscure this interaction. We hypothesized that the root hair mutant would recruit more P-cycling bacteria and AMF compared to its wild-type background to compensate for the loss of root hairs. The aims were investigated via two principal experiments. First, a field experiment compared the development of the P-cycling bacterial community and AMF colonization with and without fully developed root hairs under field conditions (GS11 and GS12-GS13). Second, a pot experiment using high- and low-P soils was used to compare the status of the P-cycling bacterial community and AMF symbiosis at booting, (GS45-GS47; Zadoks et al., 1974) when P uptake is highest (Jones et al., 2024), in the root hair mutant and wild-type.

Materials and Methods

Plant material

The wheat root hair mutant, *srh1,* and its corresponding wild-type line have been previously described (Tsang, Thomelin, et al., 2024). Briefly, the mutant was identified in a forward screen of an ethyl methanesulfonate (EMS)-mutated population created in the spring wheat cultivar Cadenza (Krasileva et al., 2017). In the mutant, root hairs initiate but fail to elongate.

Field experiment set-up and sampling

Wild-type and mutant seeds were sown in spring 2024 in a complete randomized block design in Hinxton, Cambridgeshire, United Kingdom (52°05'56.1"N, 0°10'41.8"E). The field soil characteristics are described in Table S1. Approximately 120-180 seeds were sown per plot, where each plot measured 1x1 m with 6 rows of plants per plot. Plants were excavated at two and four weeks post-sowing (GS11 and GS12-GS13, respectively; Zadoks et al., 1974). One individual plant was sampled from each replicate plot (n = 10) using a sterilized shovel, with care to take the entire root system. Following the process by described by Guan et al. (2024), plants were gently shaken to remove the loosely attached bulk soil, and only the rhizosphere (soil influenced by the root) sample was taken, as the rhizoplane soil (soil directly attached to the root) was too small to collect. The shoot length and the length of the longest root of the root system were measured. At each sampling time point, bulk soil (n = 5) was also collected from the bare soil between the plots. Samples were stored at -80 °C until freeze-drying under vacuum at -70 °C. Thereafter, the dried samples were stored at 4 °C until DNA extraction.

For each plant sampled, shoots were dried at 37 °C, and the dry weight was subsequently recorded. Roots were stored in 70% ethanol at 4 °C until root scanning. Root scans were taken using an Epson Dual Lens System Epson Perfection V800 Photo at 600 DPI in greyscale. RhizoVision Explorer version 2.0.3 (Seethepalli et al., 2021) was used to analyze the root scans to calculate total root length, average diameter, perimeter, volume, surface area, and branching frequency. Scans were taken in “Broken roots” mode and at an image thresholding level of 175. Edge smoothing was enabled with a threshold of 3, and root pruning was enabled at a threshold of 10. Non-root objects below 2 mm^2 were removed. After root scanning, the roots were dried at 37 °C, and the dry weight was subsequently recorded.

Pot experiment set-up and sampling

High- and low-P field soil was collected from the Sawyers Experimental Field site at Rothamsted Research (Harpenden, UK; 51° 48′ 59.39″ N, 0° 22′ 33.28″ W). Soils from two historically low-P plots (last measured Olsen P = 7.1 mg/kg and 5.7 mg/kg in February 2022; A. Riche, personal communication, May 1, 2024) and two historically high-P plots (last measured Olsen P = 19.3 mg/kg and 18.6 mg/kg in February 2022; A. Riche, personal communication, May 1, 2024) were collected and mixed to create the low- and high-P potting soil, respectively. The soil was sieved through 4 mm mesh and mixed with washed sand (Horticultural Silver Sand, Melcourt, Tetbury, UK) in a 3:2 ratio (w/w) to improve drainage and root aeration. Samples of the soil-sand mixture for bulk soil measurements were stored at -80 °C. Characteristics of the low- and high-P soils are listed in Table S1. Two-liter pots (12 cm H x 12 cm W x 20 cm L) were sterilized (Hortisept Pro, Conka, Nelson, UK), dried, and filled with the soil-sand mixture. Wild-type and mutant seeds were pre-germinated on moistened filter paper in the dark for three days before planting one seed per pot. Plants were grown in a climate chamber (Conviron CMP6010) under 16-hour days at 20 °C, 60% humidity, and light level 3, and 8-hour nights at 18 °C, 60% humidity for five weeks, at which the plants had reached booting stage (GS45-GS47; Zadoks et al., 1974). Throughout growth, pots were rotated twice a week and watered as needed approximately three times a week.

Plants were gently removed from the pots, and the root system was divided in half along the longitudinal axis. Approximately half the root system was used for rhizosphere and rhizoplane sampling as described in Guan et al. (2024). Rhizosphere and rhizoplane samples were stored at -80 °C until freeze-drying under vacuum at -70 °C; thereafter, the dried samples were stored at 4 °C until DNA extraction.

Shoots were dried at 37 °C and subsequently the dry weight was recorded. Roots were stored in 50% ethanol at 4 °C until AMF staining.

145 ## DNA extraction, gene quantification, and sequencing

146 DNA from up to 500 mg freeze-dried rhizosphere samples from the field experiment and
147 rhizosphere and rhizoplane samples from the pot experiment was extracted using a FastPrep-
148 24 5G beadbeating system (MP Biomedicals, Irvine, CA, USA) at 6.0 m/s for 40 s and the
149 FastDNA SPIN Kit for soil (MP Biomedicals, Irvine, CA, USA) following the manufacturer's
150 instructions. DNA quality and quantity were tested using a NanoDrop ND-1000
151 spectrophotometer (Thermo Fisher Scientific, Carlsbad, CA, USA) and a Qubit 2.0
152 Fluorometer (Thermo Fisher Scientific, Carlsbad, CA, USA), respectively. DNA was diluted
153 ten-fold to a quantity between 1 and 10 ng/µL.

154 Quantification of 16S rRNA genes and bacterial P-cycling genes (*bpp*, *phnK*, *phoD*, *phoX*, and
155 *pqqC*) in the samples was performed by qPCR using the AriaMx Real-Time PCR system
156 (Agilent Technologies, Santa Clara, CA, USA) following the methods described in Hao et al.
157 (2020). Primers are listed in Table S2. qPCR products were visualized on a 1% agarose gel
158 using GelRed (Sigma Aldrich, Denmark) to confirm amplification of the target gene. Standard
159 curves and negative controls were run in triplicate on each plate.

160 For long-read Nanopore amplicon sequencing of the 16S rRNA gene from the rhizosphere
161 samples, PCR was used to amplify 1050 bp of the 16S rRNA gene using primers 341F (5'-
162 CCTACGGGNGGCWGCAG -3') and 1391R (5'- GACGGGCGGTGWGTRCA -3') (Thijs et al.,
163 2017) using Platinum SuperFi II polymerase (Thermo Fischer Scientific, Waltham, USA). The
164 ZymoBIOMICS Microbial Community DNA Standard (Zymo Research, Irvine, CA, USA) was
165 included as a sequencing control. The PCR cycling conditions were as follows: an initial
166 denaturation step of 98 °C for 30 s, followed by 30 cycles of denaturation at 98 °C for 10 s,
167 annealing at 64 °C for 30 s, and elongation at 72 °C for 45 s, and a final elongation at 72 °C
168 for 5 m. PCR products were visualized via electrophoresis on a 1% agarose gel before
169 purification using AMPure XP beads (Beckman Coulter Inc., Brea, CA, USA) at a 0.6 ratio.
170 The sequencing library was prepared using a native barcoding kit V14 (SQK-NBD114.96) and
171 sequenced using a PromethION R10.4.1 flow cell on the PromethION P2 Solo platform
172 (Oxford Nanopore, UK). Adapter trimming and basecalling were performed using Dorado
173 version 0.7.0 using the super accurate setting (github.com/nanoporetech/dorado).

174 Seqtk (github.com/lh3/seqtk) was used to discard reads below 1000 bp and above 1500 bp.
175 Amplicon sequences were extracted from between the primer sequences using
176 strip_degen_primer_deep (github.com/padbr/asat). NanoFilt version 2.8.0 (De Coster et al.,
177 2018) was used to discard amplicon sequences with an average quality score below 25.
178 Cutadapt version 3.5 (M. Martin, 2011) was used to truncate longer reads at 1010 bp. The
179 remainder of the analysis was performed in R version 4.3.1 (R Core Team, 2023). The reads

were dereplicated to form amplicon sequence variants (ASVs) and assigned taxonomy using dada2 version 1.22.0 (Callahan et al., 2016) with the SILVA database version 138.2 (Quast et al., 2013). The ASV table was transformed to a phyloseq object for subsequent analysis using phyloseq version 1.44.0 (McMurdie & Holmes, 2013). Non-bacterial ASVs and those assigned to chloroplasts and mitochondria were discarded before the ASVs were agglomerated at the genus level while retaining non-classified reads. The Zymo mock community was used to assess sequencing contamination. Ampvis2 version 2.8.1 (Andersen et al., 2018) was used to visualize bacterial community composition. A dissimilarity matrix was calculated with rarefaction using avgdist() from the vegan package version 2.6-4 with default parameters (vegandevs.github.io/vegan). The rarefied dissimilarity matrix was used to generate the principal coordinate analysis based on Bray-Curtis dissimilarities and to run a PERMANOVA using adonis2() from vegan. Pairwise comparisons were made with the package pairwiseAdonis version 0.4.1 (github.com/pmartinezarbizu/pairwiseAdonis). The Shannon diversity index (alpha diversity) was calculated after rarefaction 100 times, as proposed by Schloss, 2024. Briefly, the dataset was rarefied, and the Shannon diversity index was subsequently calculated as the mean Shannon diversity index over 100 replicates. Differentially abundant ASVs between the mutant and wild-type were generated using corncob version 0.4.1 (B. D. Martin et al., 2020) with a false discovery rate of 0.05.

Raw reads are deposited in NCBI under BioProject PRJNA1308004.

P content of soil and shoots

Bulk soils from the field and pot experiment were analyzed for pH, Olsen extractable P, and ammonium nitrate extractable potassium (K) and magnesium (Mg) by NRM Cawood Scientific (Bracknell, UK). The bulk soil from the field trial had a pH of 7.8 and an Olsen extractable P content of 12.8 mg/L (Table S1). In the pot experiment, the low-P soil had an Olsen extractable P content of 10.0 mg/L, and the high-P was slightly higher at 13.7 mg/L (Table S1).

Dried shoots were homogenized and ground using a zirconium ball mill, and the P concentration was determined using the dry ashing method of Saunders & Williams (1955) followed by the molybdate-blue method (Murphy & Riley, 1962) using flow injection analysis (FIAstar 5000 analyzer, Foss, Hillerod, Denmark). Briefly, 100 mg samples were placed in acid-washed crucibles and ashed in a muffle furnace at 550 °C for one hour. The ash was mixed with 50 mL 0.5 M sulfuric acid and shaken overnight at room temperature. Extracts were filtered through ashless filters (Whatman No. 42), and samples were diluted 10X before analysis. Two blanks and one replicate of the standard reference material 1515 (NIST 1991) (Sigma Aldrich, Denmark) were included in the analysis.

214 ## AMF quantification

215 Due to the small and fragile root system of the field-grown plants, relative qPCR was used to
216 quantify AMF colonization (Bodenhausen et al., 2021). DNA was extracted from the dried field-
217 grown roots using a FastPrep-24 5G beadbeating system (MP Biomedicals, Irvine, CA, USA)
218 at 6.0 m/s for 40 s and the FastDNA SPIN Kit (MP Biomedicals, Irvine, CA, USA) following the
219 manufacturer's instructions. DNA quality and quantity were tested as described above. DNA
220 was diluted ten-fold to a concentration between 1 and 10 ng/µL. AMF colonization was
221 quantified using the 18S rRNA gene fragment, amplified with the AMF-specific primers AMG1F
222 (Hewins et al., 2015) and AM1 (Helgason et al., 1998) (Table S2) on an AriaMx Real-Time
223 PCR system (Agilent Technologies, Santa Clara, CA, USA). The PCR program consisted of
224 an initial denaturation step of 15 min at 95 °C, followed by 45 cycles of denaturation at 95 °C
225 for 15 s, annealing at 62 °C for 30 s, and elongation at 72 °C for 20 s followed by a melting
226 curve analysis (from 65 to 95 °C, with 0.5 °C steps holding for 5 s) (Bodenhausen et al., 2021).
227 The AMF 18S rRNA gene signal was normalized using a wheat gene encoding a
228 heterogenous nuclear ribonucleoprotein Q, *hn-RNP-Q*, which was amplified with previously
229 described primers (Qi et al., 2012) (Table S2). The PCR program consisted of an initial
230 denaturation of 3 min at 95 °C, followed by 40 cycles of denaturation at 94 °C for 15 s,
231 annealing at 58 °C for 15 s, and elongation at 72 °C for 20 s followed by a melting curve
232 analysis (from 61 to 95 °C, with 0.5 °C steps holding for 5 s). For both primer sets, each 20 µL
233 qPCR reaction contained 10 µL 2X Brilliant III Ultra-Fast SYBR Green qPCR Master Mix with
234 Low ROX (Agilent Technologies, Santa Clara, CA, USA), 0.4 µM each of forward and reverse
235 primer, 1 mg/mL bovine serum albumin (New England Bioabs, MA, USA), and 2 µL of template
236 DNA. qPCR products were visualized on a 1% agarose gel to confirm amplification of the
237 target gene. Negative controls were run in triplicate for each primer pair. Raw fluorescence
238 data were imported to LinRegPCR (version 2021.2) (Ruijter et al., 2009) to determine cycle
239 number to threshold (Ct) and efficiency (*E*) using the default baseline threshold from
240 LinRegPCR. The AMF 18S rRNA gene signal was normalized to plant DNA as described by
241 Bodenhausen et al. (2021).

242 In the pot experiment, AMF colonization was quantified via staining. From each plant,
243 approximately 1-2 cm of the middle of the root was taken for AMF staining with Trypan Blue.
244 Root samples were incubated in 2 mL microcentrifuge tubes containing 2 mL 10% KOH for 25
245 min at 90˚C. Subsequently, the KOH was removed, and the roots were washed twice with
246 distilled water. After washing, roots were incubated in 2 mL 0.3 M HCl for 30 min at room
247 temperature. After removing the HCl, roots were incubated in 2 mL 0.1% Trypan Blue stain for
248 eight minutes at 90˚C. Roots were then washed twice with acidic glycerol (1:1 glycerol:0.3 M
249 HCl v/v) and incubated with the last wash overnight at room temperature in the dark. No fewer

250 than ten stained root sections per sample were mounted on microscope slides. Scoring for
251 AMF presence and arbuscule formation was performed on 100 fields of view per slide using a
252 Leica DMLS microscope (Leica Microsystems, Wetzlar, Germany) under 200X magnification
253 (Brundrett et al., 1996).

254 ### Statistical analysis

255 Data analysis was conducted in R version 4.3.1 (R Core Team, 2023), and all plots were
256 created using ggplot2 version 3.5.1 (Wickham, 2016). Significance was defined as $p < 0.05$.
257 Before linear model generation, the appropriate data transformation was identified using the
258 Box-Cox transformation. All analyses of variance (ANOVAs) were performed using the car
259 package version 3.0-5 (Fox & Weisberg, 2019) unless stated otherwise. All post-hoc pairwise
260 comparisons were performed using the emmeans package version 1.10.4
261 (rvlenth.github.io/emmeans) with Tukey's Honestly Significant Difference (HSD) test. When
262 applicable, the Benjamini & Hochberg method (Benjamini & Hochberg, 1995) was used to
263 correct for multiple testing.

264 For field-grown plant parameters, the Shapiro-Wilk test was used to check for normality
265 between means. The Welch Two Sample t-test was used to compare means for parametric
266 groups, while the Wilcox test was used for non-parametric groups. For AMF colonization in
267 the field-grown plants, a linear model was used to assess the effects of sampling time point
268 and genotype on long-transformed normalized AMF gene signal, followed by a two-way
269 ANOVA.

270 For pot-grown plant parameters and AMF colonization, a linear model was used to assess the
271 effects of genotype and soil P status, followed by a two-way ANOVA. The AMF colonization
272 data were square root transformed and shoot dry weight data was log transformed prior to
273 analysis. Due to the presence of zero count data in the arbuscule dataset, an aligned ranks
274 transformation (ART) ANOVA was used as a non-parametric approach via the ARTool
275 package version 0.11.1 (Kay et al., 2021).

276 All bacterial P-cycling qPCR data were log-transformed before analysis. For the field qPCR
277 data, a linear model was used to assess the effects of sampling time point and sample source
278 (root hair mutant, wild-type, or bulk soil) on gene relative abundance, followed by a two-way
279 ANOVA. For the high- and low-P qPCR data, a linear model was used to assess the effects
280 of genotype, soil condition, and rhizocompartment on gene relative abundance, followed by a
281 three-way ANOVA.

Results

The loss of root hair elongation stunted root system growth in the field only at the early seedling developmental stage

As a preliminary check to confirm the mutant phenotype, the mutant plants were visually assessed for root hair growth. This confirmed that the phenotype of arrested root hair elongation was apparent in a natural soil environment at GS11, GS12-GS13, and GS45-GS47. Importantly, root hair elongation was not stimulated in the mutant under low-P conditions (Figure S1).

To assess the effect of the *srh1* mutation on overall plant development under agricultural settings, ten growth parameters of the field-grown plants were measured. At two weeks post-sowing (GS11), the mutant had a smaller root system as defined by root dry weight, total root length, average diameter, perimeter, volume, surface area, and branching frequency (Figure 1). However, aboveground growth characteristics were unaffected (Figure 1A-B). At four weeks post-sowing (GS12-13), no difference was observed between the plants of the mutant and wild-type across all ten phenotypic parameters (Figure 1).

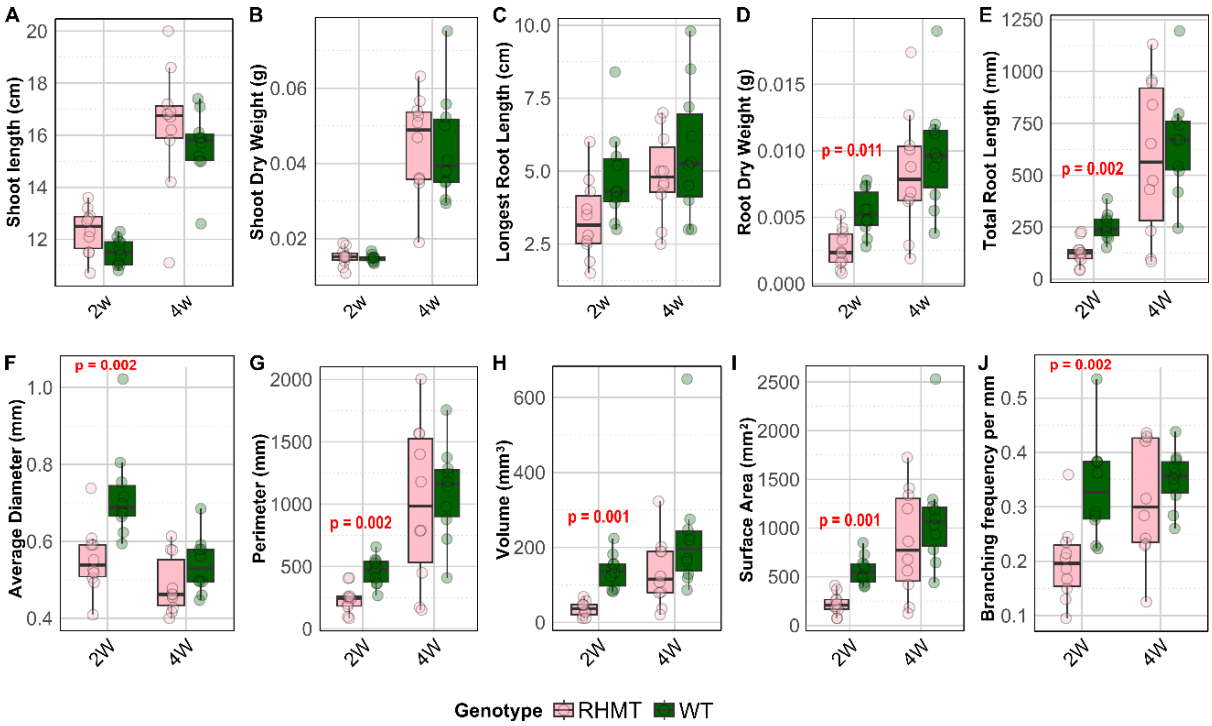

Figure 1. Root hair mutant (RHMT) and wild-type (WT) phenotypic parameters measured from field-grown plants, sampled at two (2W, n = 10) and four weeks (4W, n = 9) post-sowing. The boxplots display the median, the two hinges (25th and 75th percentile), and the upper and lower whiskers (extending to the largest and smallest values no further than 1.5 times the interquartile range). True data points are overlaid on the boxplots as filled circles. P-

303 values were calculated using the Wilcox test and adjusted for multiple testing using the
304 Benjamini & Hochberg method. Significant differences between means (p-values < 0.05) are
305 shown in red.

306 The wheat root hair mutant showed a temporal shift from enrichment of bacterial P
307 mineralization genes to AMF colonization in the field

308 The ability of the root hair mutant to enrich its bacterial microbiome for P mobilization was
309 assessed using qPCR on DNA extracted from samples collected under field conditions across
310 early seedling development. The relative abundance of all bacterial P-cycling genes analyzed,
311 except for *phoX,* was affected by sample source (root hair mutant, wild-type, or bulk soil) ($p <$
312 0.05). Neither sampling time point nor the interaction between sample source and sampling
313 time point influenced the relative abundance of the tested genes ($p > 0.05$). (Table 1).

314 At two weeks post-sowing, bacterial genes involved in organic P mineralization (*bpp* (beta-
315 propeller phytase), *phnK* (phosphonate degradation), and *phoD* (cytoplasmic phosphatase))
316 were enriched in the rhizosphere of the root hair mutant compared to wild-type (Table 1A).
317 The root hair mutant rhizosphere was enriched in these genes compared to the bulk soil, while
318 the relative abundance in the wild-type rhizosphere was similar to that of the bulk soil. The
319 levels of *phoX* (periplasmic phosphatase) and *pqqC* (pyrroloquinoline-quinone synthase) were
320 no different between the root hair mutant and wild-type. The relative abundance of the *pqqC*
321 gene was lower in the rhizosphere of both genotypes compared to the bulk soil.

322 At four weeks post-sowing, there was no enrichment of any of the targeted genes in the
323 rhizosphere of the root hair mutant compared to the wild-type (Table 1B). The relative
324 abundance of *bpp*, *phnK,* and *phoD* in the rhizosphere of the root hair mutant dropped to
325 match that of wild-type. Nevertheless, at this time point, the relative abundance of the *bpp*
326 gene was still higher in the rhizosphere of both genotypes compared to the bulk soil. The
327 relative abundance of the *pqqC* gene was still lower in the rhizosphere of both genotypes
328 compared to the bulk soil at this time point.

Age	Genotype	*bpp*		*phnK*		*phoD*		*phoX*		*pqqC*	
2W	**RHMT**	1.14e-3 ± 7.05e-4	a	2.52e-1 ± 1.91e-1	a	2.77e-1 ± 2.56e-1	a	4.03e-2 ± 1.05e-2	a	3.75e-3 ± 2.83e-3	a
2W	**WT**	5.73e-4 ± 1.17e-4	b	1.21e-1 ± 2.32e-2	b	7.75e-2 ± 9.24e-3	b	4.28e-2 ± 7.21e-3	a	1.83e-3 ± 3.74e-4	a
2W	**Bulk Soil**	5.09e-4 ± 1.01e-4	b	1.10e-1 ± 2.92e-2	b	1.05e-1 ± 2.27e-2	ab	5.72e-2 ± 1.85e-2	a	6.42e-3 ± 2.00e-3	b
4W	**RHMT**	8.23e-4 ± 4.35e-4	a	1.82e-1 ± 1.32e-1	a	1.54e-1 ± 2.18e-1	a	4.50e-2 ± 1.16e-2	a	2.50e-3 ± 2.00e-3	a
4W	**WT**	6.31e-4 ± 1.63e-4	a	1.19e-1 ± 2.33e-2	ab	7.27e-2 ± 1.30e-2	a	4.69e-2 ± 1.50e-2	a	1.86e-3 ± 4.24e-4	a
4W	**Bulk Soil**	3.66e-4 ± 9.49e-5	b	8.31e-2 ± 1.05e-2	b	8.56e-2 ± 1.84e-2	a	4.81e-2 ± 1.28e-2	a	5.56e-3 ± 1.64e-3	b

Table 1. Relative abundance of bacterial P-cycling genes in root hair mutant (RHMT) and wild-type (WT) plants grown in the field and sampled at two weeks post-sowing (2W, n = 10) and four weeks post-sowing (4W, n = 9). Relative abundance was calculated by normalizing gene copy number to the 16S rRNA gene copy number in each sample measured by qPCR. Data are presented as the mean ± standard deviation. Bulk soil samples were from bare soil between the plots (no plant, n = 5). Means that share the same letter within each gene in each time point are not statistically different (Tukey's HSD, $p < 0.05$).

AMF colonization in the field was quantified by qPCR on DNA extracted from the roots of the field-grown plants. There was no effect of genotype nor interaction between genotype and age ($p > 0.05$). However, there was an effect of plant age ($p < 0.05$); the plants sampled two weeks after sowing were colonized by AMF to a lesser extent than the plants sampled four weeks after sowing (Figure 2).

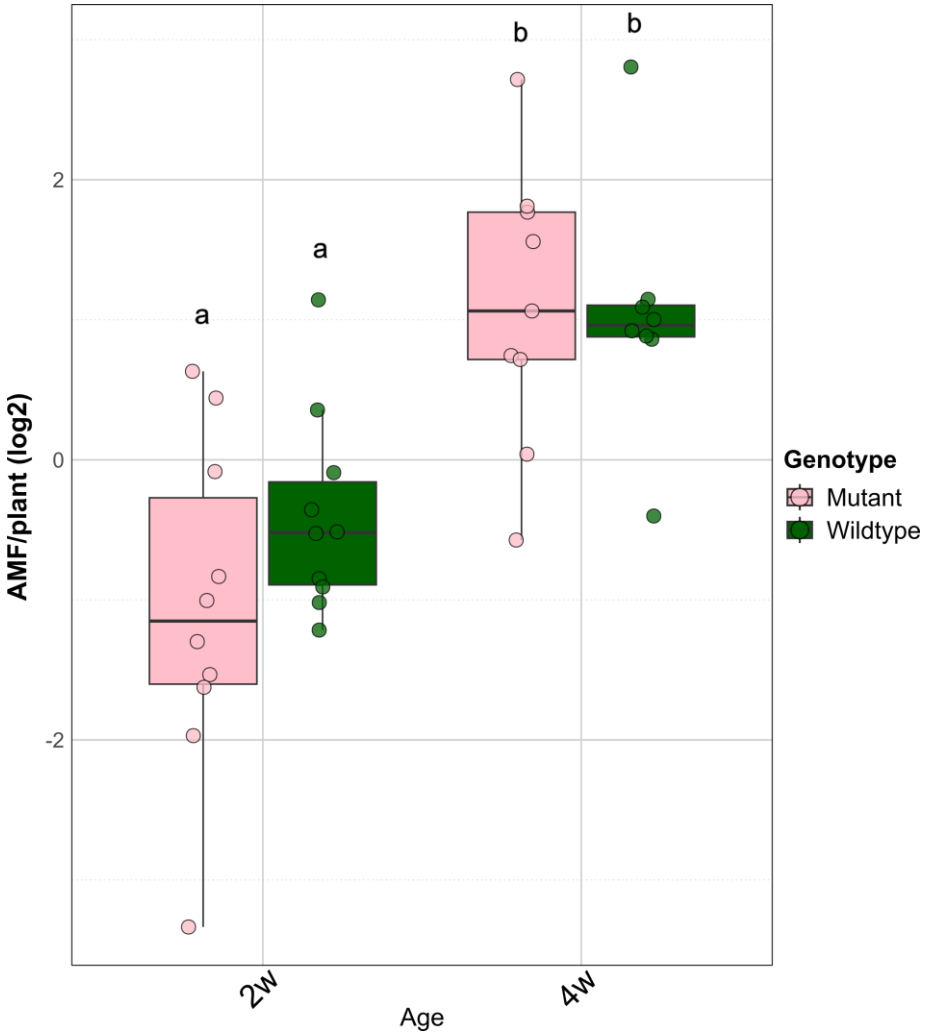

Figure 2. AMF signal quantified via qPCR and normalized to plant DNA in field-grown root hair mutant (RHMT) and wild-type (WT) plants two weeks (2W) and four weeks (4W) after sowing. The boxplots display the median, the two hinges (25th and 75th percentile), and the upper and lower whiskers (extending to the largest and smallest values no further than 1.5 times the interquartile range). True data points are overlaid on the boxplots as filled circles. Means that share the same letter are not statistically different (Tukey's HSD, $p < 0.05$).

Low-P soil status stunted aboveground plant parameters at booting in the presence and absence of root hair elongation

To compare recruitment of bacterial P-cycling genes and AMF colonization at booting and under various levels of P fertilization, the root hair mutant and wild-type were grown in pots with field soils derived from plots with contrasting P fertilization levels and sampled at booting. To ensure the effect of the high- and low-P soils was realized, plant shoot growth and P content was measured at the time of sampling (Figure 3). Soil P status and genotype affected shoot length, shoot dry weight, and shoot P concentration ($p < 0.05$), but there was no interaction between soil P status and genotype.

357 Regardless of genotype, plants in the low-P soils had smaller shoot length (Figure 3A), shoot
358 biomass (Figure 3B) and shoot P concentration (Figure 3C) than in the high-P treatment.
359 Biomass in the low-P soil was less than half of what was reached in the high-P soil. In the
360 high-P soil, the wild-type shoots grew better than the root hair mutant, while the two genotypes
361 were not different under low-P conditions (Figure 3A-B). There was no difference in P
362 concentration between the two genotypes when grown in the same soil (Figure 3C).

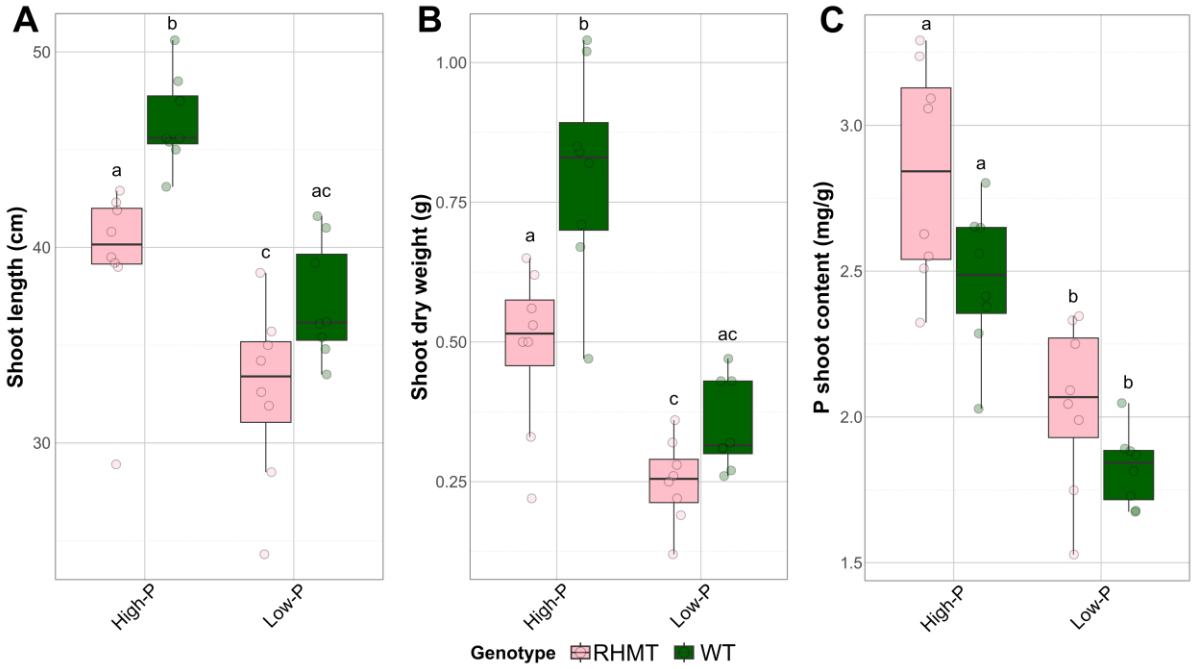

363

364 **Figure 3. Aboveground wheat growth parameters are affected by root hair mutation and**
365 **soil P status at booting.** Shoot length (A), shoot dry weight (B), and shoot P concentration
366 (C) for the root hair mutant (RHMT) and wild-type (WT) plants grown in high- and low-P soil.
367 The boxplots display the median, the two hinges (25th and 75th percentile), and the upper and
368 lower whiskers (extending to the largest and smallest values no further than 1.5 times the
369 interquartile range). True data points are overlaid on the boxplots as filled circles. Means that
370 share the same letter within each plot are not statistically different (Tukey's HSD, $p < 0.05$).

371 At booting, the root hair mutant enhanced arbuscule formation but not bacterial P-cycling
372 genes under low- and high-P conditions

373 The relative abundances of the bacterial P-cycling genes were first assessed in the bulk high-
374 and low-P soils to determine the effect of soil fertilization history on the bacterial P-cycling
375 community. The relative abundances of all the targeted bacterial P-cycling genes were greater
376 in the high-P soil compared to the low-P soil (Table 2A).

377 In the plant-associated soils, there was an effect of soil P status and rhizocompartment (i.e.
378 rhizoplane or rhizosphere) but not genotype on the relative abundances of *phoX*, *phoD*, and

379 *pqqC* ($p < 0.05$). The relative abundance of *bpp* was only affected by genotype ($p < 0.05$). No
380 factors had an impact on the relative abundance of *phnK*. Regardless of rhizocompartment or
381 soil P status, there was no enrichment of any of the bacterial P-cycling genes in the root hair
382 mutant compared to the wild-type at booting (GS45-GS47) (Table 2B). Relative abundance in
383 the rhizosphere and rhizoplane was only different between high- and low-P conditions for the
384 genes *phoD*, *phoX*, and *pqqC* (Table 2). The relative abundances of the *bpp* and *phnK* genes
385 in the rhizosphere and rhizoplane were equal between high- and low-P soils (Table 2).

Compartment	Genotype	Condition	*bpp*		*phnK*		*phoD*		*phoX*		*pqqC*	
Plane	**RHMT**	**LowP**	2.16e-4 ± 1.76e-4	a	1.39e-1 ± 5.26e-2	a	2.79e-1 ± 5.95e-2	a	8.35e-4 ± 4.13e-4	a	2.29e-3 ± 8.94e-4	ab
Plane	**WT**	**LowP**	8.17e-4 ± 1.64e-3	a	1.56e-1 ± 5.46e-2	a	3.69e-1 ± 1.73e-1	a	8.68e-4 ± 4.00e-4	a	2.42e-3 ± 5.17e-4	ac
Plane	**RHMT**	**HighP**	2.57e-4 ± 6.97e-5	a	1.49e-1 ± 6.19e-2	a	4.89e-1 ± 1.27e-1	b	1.70e-3 ± 7.66e-4	b	3.40e-3 ± 1.22e-3	cd
Plane	**WT**	**HighP**	3.09e-4 ± 1.24e-4	a	1.52e-1 ± 5.27e-2	a	5.20e-1 ± 1.20e-1	b	1.71e-3 ± 7.52e-4	b	3.63e-3 ± 2.29e-3	bd
Sphere	**RHMT**	**LowP**	2.05e-4 ± 8.29e-5	a	1.49e-1 ± 5.06e-2	a	4.29e-2 ± 1.44e-2	a	1.46e-2 ± 6.55e-3	a	4.30e-3 ± 2.31e-3	ab
Sphere	**WT**	**LowP**	2.27e-4 ± 3.32e-5	a	1.47e-1 ± 4.13e-2	a	4.17e-2 ± 1.42e-2	a	1.32e-2 ± 4.36e-3	a	4.35e-3 ± 2.10e-3	ac
Sphere	**RHMT**	**HighP**	2.18e-4 ± 4.12e-5	a	1.45e-1 ± 4.30e-2	a	6.26e-2 ± 1.57e-2	b	3.24e-2 ± 1.06e-2	b	5.19e-3 ± 2.33e-3	cd
Sphere	**WT**	**HighP**	2.07e-4 ± 3.72e-5	a	1.81e-1 ± 3.40e-2	a	6.85e-2 ± 1.72e-2	b	4.02e-2 ± 1.42e-2	b	5.47e-3 ± 1.94e-3	bd
Bulk Soil		**LowP**	1.07e-4 ± 1.19e-5	b	7.22e-2 ± 9.72e-3	b	2.04e-1 ± 2.73e-2	b	2.58e-4 ± 5.95e-5	b	1.34e-3 ± 1.56e-4	b
Bulk Soil		**HighP**	2.31e-4 ± 6.75e-5	a	1.71e-1 ± 7.06e-2	a	4.66e-1 ± 1.49e-1	a	2.00e-3 ± 1.03e-3	a	2.68e-3 ± 1.02e-3	a

386 **Table 2. Relative abundance of bacterial P-cycling genes in root hair mutant (RHMT)**
387 **and wild-type (WT) plants grown under high-P and low-P soil conditions at booting in**
388 **the rhizoplane (plane, n = 8) and rhizosphere (sphere, n = 8), and in the bulk soil controls**
389 **(n = 5).** Relative abundance is calculated by normalizing the gene copy number to the 16S
390 rRNA gene copy number in each sample measured by qPCR. Data are presented as the mean
391 ± standard deviation. Means that share the same letter within each gene in each compartment
392 are not statistically different (Tukey's HSD, $p < 0.05$).

393 AMF staining revealed the extent of AMF colonization and arbuscule formation of the roots in
394 pot-grown plants at booting (Figure 4). Genotype, soil P status, and the interaction between

395 the two factors affected total AMF colonization ($p < 0.05$). Likewise, arbuscule formation was
396 influenced by genotype and soil P status but not the interaction between the two factors ($p <$
397 0.05). Under high-P, the root hair mutant harbored more AMF than the wild-type, while at low-
398 P, the colonization levels of the two genotypes were equal (Figure 4A). With regards to
399 arbuscule formation, the root hair mutant harbored a greater percentage of arbuscules than
400 the wild-type under both high- and low-P conditions (Figure 4B). Both genotypes displayed
401 greater arbuscule formation under low-P than high-P soil status (Figure 4B).

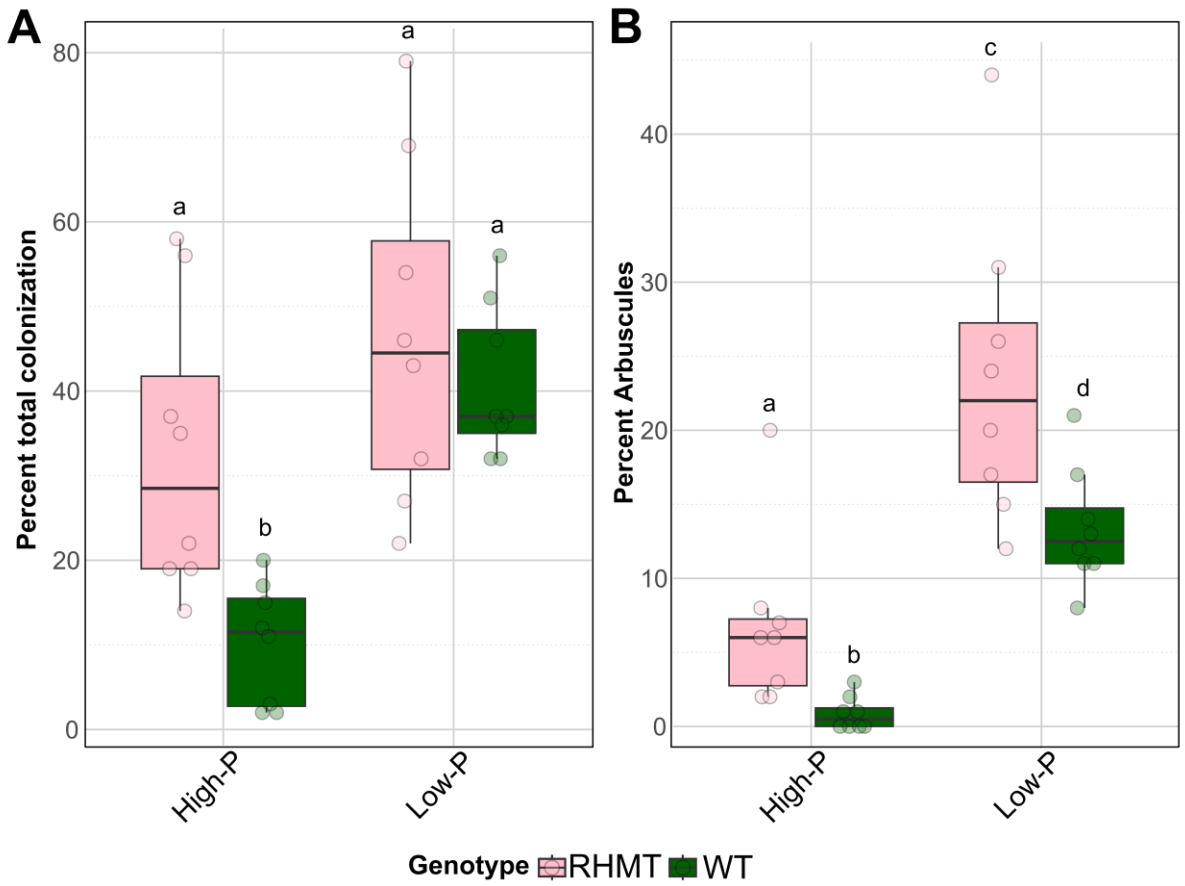

402

403 **Figure 4. Total arbuscular mycorrhizal fungi (AMF) colonization (A) and arbuscule**
404 **formation (B) in wild-type (WT) and root hair mutant (RHMT) plants grown in pots under**
405 **high- and low-P conditions at booting.** The boxplots display the median, the two hinges
406 (25th and 75th percentile), and the upper and lower whiskers (extending to the largest and
407 smallest values no further than 1.5 times the interquartile range). True data points are overlaid
408 on the boxplots as filled circles. Means that share the same letter within each plot are not
409 statistically different (Tukey's HSD, $p < 0.05$).

410 Rhizosphere bacterial community composition was shaped by the lack of root hair elongation
411 in older plants

412 To reveal the rhizosphere bacterial community taxonomic composition, long-read 16S rRNA
413 amplicon sequencing was performed on the rhizosphere of field- and pot-grown plants. After

filtering, 1,264,834 reads were retained across the two sequencing datasets. Across the field-grown plants, 677,509 reads were assigned to 1,337 ASVs, and 80.2% of ASVs were identified at the genus level. The median reads per sample was 14,621. Across the pot-grown plants, 587,325 reads were assigned to 1,263 ASVs, with 80.5% of the ASVs identified at the genus level. The median reads per sample was 14,519.5.

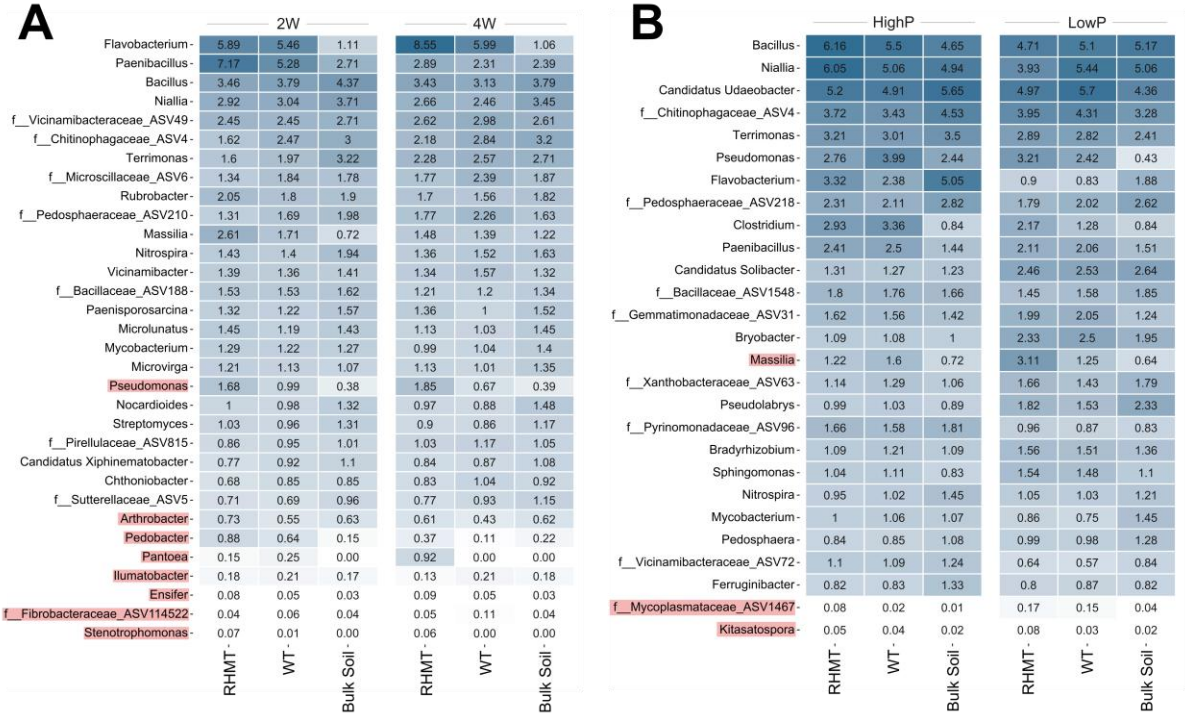

Figure 5. The relative abundance of the top 25 bacterial genera, plus genera identified as differentially abundant between the root hair mutant (RHMT) and wild-type (WT), highlighted in red, in the rhizosphere of field-grown plants (A) and pot-grown plants (B) compared to bulk soil. The heatmap displays the mean relative abundances of the samples within a treatment: two weeks post-sowing (2W) mutant (n = 10) and wild-type (n = 9); four weeks post-sowing (4W) mutant (n = 10) and wild-type (n = 8); booting in high-P soil (HighP) mutant (n = 8) and wild-type (n = 8); booting in low-P soil (LowP) mutant (n = 6) and wild-type (n = 6). Bulk soil samples were taken from unplanted soil (n = 5).

For the field-grown plants, long-read 16S rRNA amplicon sequencing identified an impact of genotype (PERMANOVA, $p = 0.020$, $R^2 = 0.06$) and age (PERMANOVA, $p = 0.001$, $R^2 = 0.11$) on the bacterial community in the rhizosphere (Figure S2A). Pairwise comparisons between the genotypes at two- and four-weeks post-sowing revealed that only the microbiome of four-week-old plants were different ($p = 0.031$). Indeed, there were no bacterial genera that were enriched in one genotype or the other at two weeks post-sowing. On the other hand, at four weeks post-sowing, *Ilumatobacter* and an unidentified genus of the Fibrobacteraceae family were enriched in wild-type plants, while *Arthrobacter, Ensifer*, *Pseudomonas*,

436 *Stenotrophomonas*, *Pedobacter*, and *Pantoea* were enriched in the mutant (Figure 5A, Figure
437 S2B). Alpha diversity of the microbiome was not different between the wild-type and the
438 mutant at either sampling time point (Figure S2C).

439 In the pot-grown plants, soil P status (PERMANOVA, $p = 0.001$, $R^2 = 0.36$) and the interaction
440 between genotype and soil P status (PERMANOVA, $p = 0.014$, $R^2 = 0.07$) impacted the
441 bacterial microbiome in the rhizosphere (Figure S2D). Pairwise comparisons revealed that the
442 rhizosphere microbiome of the mutant and wild-type were different under both high- and low-
443 P conditions ($p = 0.036$ and $= 0.029$, respectively). Under high-P soil conditions, an unknown
444 genus of the Mycoplasmataceae family was enriched in the mutant (Figure 5B, Figure S2E).
445 Under low-P conditions, the genera *Massilia* and *Kitasatospora* were enriched in the mutant
446 (Figure 5B, Figure S2E). There were no taxa differentially enriched in the wild-type in either
447 soil. Alpha diversity of the microbiome was not different between the wild-type and the mutant
448 in either high-P or low-P conditions (Figure S2F).

449 Discussion

450 The potential of the plant to utilize its bacterial and fungal microbiome for P nutrition has yet
451 to be fully understood. In this work, we used a novel root hair mutant in wheat to reduce the
452 dominance of root hair plasticity response in P uptake so that the ability of wheat to exploit the
453 soil microbiome for P nutrition can be revealed. We tested the hypothesis that the root hair
454 mutant would boost recruitment of P-cycling bacteria and AMF to compensate for the loss of
455 root hair elongation.

456 The phenotype of arrested root hair elongation was maintained in the root hair mutant at each
457 growth stage and under all conditions studied. We found a stunting effect of the *srh1* mutation
458 on early root system development, which was mirrored by diminished aboveground biomass
459 at booting (GS45-GS47). Reduced root growth and development is typical of hairless mutants
460 in other crop species grown in soil, highlighting the importance of root hairs in overall crop
461 development (Haling et al., 2013; Ma et al., 2020; Suzuki et al., 2003). In the wheat root hair
462 mutant, it is unlikely that the stunting effect of the *srh1* mutation was solely due to impaired
463 nutrient acquisition, as the shoot P content of the mutant was similar to the wild-type.
464 Nevertheless, despite potential pleiotropic effects of the mutation on crop growth, the inhibition
465 of root hair elongation in the mutant is a useful tool to test our hypothesis.

466 We demonstrate that loss of root hair elongation affects the P-cycling bacterial community
467 during early wheat development under field conditions. We establish support for our
468 hypothesis that the root hair mutant can enrich bacterial P mineralization genes in the
469 rhizosphere under field conditions compared to the wild-type. Relative abundance of the P

solubilization-related gene *pqqC*, the co-factor for gluconic acid production (An & Moe, 2016), was no different between the root hair mutant and wild-type. Since plants normally rely on root hairs to mobilize organic P into orthophosphate anions (Gahoonia et al., 2001; Ma et al., 2020; Richardson et al., 2011), the specific enrichment of bacterial organic P mineralization genes in the root hair mutant suggests a bacterial route for organic P acquisition to compensate for the loss of root hairs. Indeed, bacteria that metabolize plant root exudates play a significant role in organic P mineralization in the soil (Wang et al., 2025), indicating a potential relationship between microbial function and plant needs. While we cannot rule out competition for P between bacteria and the plant (Raymond et al., 2021), niche-filling in the rhizosphere of the root hair mutant would arguably enrich all P-bacterial cycling genes, not selectively mineralization, as competitors for P in the soil proliferate in the carbon-rich rhizosphere.

However, bacterial P mineralization genes were only enriched in the root hair mutant at two weeks post-sowing. Sampling two weeks later at GS12-GS13 revealed that the relative abundance of organic P mineralization genes in the root hair mutant rhizosphere dropped to match that of the wild-type. While P uptake in the first weeks of growth plays a vital role in seedling establishment and vigor (Yi et al., 2023), the rate of P uptake in wheat reaches its maximum during booting (Jones et al., 2024). Thus, regardless of the loss of enrichment of bacterial P cycling genes in the mutant at four weeks post-sowing (GS12-GS13) in the field, we still expected to see enrichment of P-cycling genes in the mutant at booting, particularly in the low-P soil. However, this hypothesis was not supported; at booting (GS45-GS47) in the pot experiment, relative abundances of all bacterial P-cycling genes were no different between the mutant and wild-type. Soil P affected bacterial P-cycling gene relative abundance regardless of root hair status. Previously, high P inputs have been shown to promote the ability of bacteria to interact with soil P (Dai et al., 2020; Xiao et al., 2022). Nevertheless, since two different soils were used in the field and pot experiments, direct comparisons of the bacterial P mineralization response to the root hair mutant between these experiments must be carefully interpreted. Ideally, measurements of organic P in the field versus the pots would provide further insights into how organic P conditions in the soil may influence the responsiveness of organic P mineralization genes in the rhizosphere of the root hair mutant.

Root morphology plays a role in structuring the rhizosphere microbiome (Saleem et al., 2018; Herms et al., 2022). Indeed, there was a tangible effect of the loss of root hairs on bacterial community composition, but we could not see meaningful links between the long-read 16S rRNA amplicon sequencing and the bacterial qPCR results. That is, differences between the root hair mutant and wild-type in community composition were only apparent in older plants, while P-cycling capabilities only differed between the youngest plants. This disparity between compositional and functional differences was likely because 16S rRNA sequences, even full-

length, are poor proxies for functional capabilities (Jaspers & Overmann, 2004), a statement we have also found to be true in wheat rhizosphere *Pseudomonas* isolates (Herms et al., 2025). Thus, taxonomic profiling is insufficiently sensitive to reveal P-cycling capabilities, and we therefore prioritize the results of the qPCR analyses for interpretation of P-cycling. Nevertheless, we still provide evidence for the role of root hairs in shaping the bacterial community in the wheat rhizosphere, especially as the plants matured, as found in barley and maize (Quattrone et al., 2024; Robertson-Albertyn et al., 2017). This can be attributed to the loss of unique colonization niches (Buddrus-Schiemann et al., 2010; Mousa et al., 2016) or altered root exudate profiles compared to their wild-type background (Galloway et al., 2022; Lohse et al., 2023; Sasse et al., 2018). Analysis of the root exudates of the wheat root hair mutant, while out of scope in this work, could help clarify this dysbiosis.

The drop in bacterial P mineralization genes at GS12-GS13 in the root hair mutant coincided with a marked increase in AMF colonization levels across the plants from GS11 to GS12-GS13. This agrees with previous work that found AMF colonization in field-grown wheat to be lacking until GS12 (Marrassini et al., 2024). The root system needs to be sufficiently developed before the AMF symbiosis can be initiated (Werner & Kiers, 2015). We saw that root growth of the mutant matched that of the wild-type at GS12, potentially indicating a readiness for AMF colonization or, alternatively, a direct root response to AMF colonization (Zhu et al., 2025). Collectively, these findings indicate a temporal shift from enrichment of bacterial P-cycling to dominance of the AMF symbiosis. In support of this, we observed no enrichment of bacterial P-cycling genes in the root hair mutant compared to the wild-type at booting (GS45-GS47), when P uptake is highest in wheat (Jones et al., 2024), nor when we induced additional P stress via cultivation in low-P soil. At GS45-GS47, the roots were also heavily colonized by AMF. However, since this work took place across two different soils, the AMF communities, colonization potential, and responsiveness may be different between the field and the pots (Jansa et al., 2014) and direct parallels between the experiments must be interpreted with caution. Taken together, our results suggest that before the AMF symbiosis is fully dominant, wheat can recruit and rely on bacterial P mineralization to meet their P needs and then release these bacterial players once the AMF symbiosis is developed.

It is well known that plants, including wheat, enrich AMF colonization when grown under limited P (Kumar et al., 2019; Zhou et al., 2022; Wang et al., 2025). Root hair mutants in barely and maize also display a similar response of increased AMF colonization, likely as a compensatory mechanism for nutrient uptake in the absence of root hairs (Jakobsen et al., 2005; Kumar et al., 2019; Ma et al., 2020). Our results add further evidence to the conserved ability of cereal crops to increase AMF recruitment when root hair development is inhibited. Notably, we saw higher arbuscule formation in the root hair mutant, regardless of soil P status. Arbuscules are

542 the specialized mycorrhizal structures that facilitate mineral nutrient translocation from fungus
543 to plant (Smith & Smith, 2011). This result indicates not only enhanced colonization by AMF,
544 but also a reliance of the root hair mutant on AMF for mineral P uptake. This further supports
545 our claim that in the root hair mutant, AMF replace P mineralizing bacteria as the root system
546 develops. Ideally, quantifying plant P stress across developmental stages when the crop is
547 grown only with P-cycling bacteria or only with AMF would solidify the importance of these
548 microorganisms in wheat P uptake.

549 Our results also indicate that AMF may play a greater role than root hairs in wheat performance
550 under low-P conditions. In the field and in high-P soil, the root hair mutant had stunted growth
551 compared to the wild-type, as expected (Haling et al., 2013; Ma et al., 2020; Suzuki et al.,
552 2003). However, under low-P conditions, there was no difference in biomass or shoot P
553 content between the two genotypes at booting. The combination of the loss of root hairs with
554 low-P soil should increase the stress of the plant (Gahoonia et al., 2001), but the root hair
555 mutant coped relatively well. Under low-P, the root hair mutant boasts high AMF colonization
556 and increased arbuscule formation. Taken together, these results suggest the greater
557 influence of AMF compared to root hairs in wheat P nutrition. Similar conclusions have been
558 made in maize, where inoculation of a root hairless mutant with AMF in low-P conditions
559 resulted in better performance than the wild-type grown under the same conditions (Ma et al.,
560 2020).

561 Despite decades of research, successfully manipulating the rhizosphere microbiome for
562 improved crop nutrition remains limited. Our results shed light on how wheat roots deficient in
563 root hairs rely on bacterial and fungal partners for P nutrition. A practical implication of this
564 finding is that, given genotypic variation in root hair length within elite wheat germplasm
565 (Delhaize et al., 2015), the genotypes with constitutively short root hairs or poor plasticity
566 (Nguyen & Stangoulis, 2019) are likely to enlist microbial mechanisms to ensure P nutrition.
567 Collectively, this work can be used to guide improvements of the microbial P uptake
568 mechanisms in wheat. By considering the natural ecology in the rhizosphere of the root hair
569 mutant, we recommend focusing on bacterial interactions only during the early stages of wheat
570 development and otherwise prioritizing the AMF symbiosis throughout wheat growth.

571 Acknowledgements

572 The authors thank Andrew Riche (Rothamsted Research, Harpenden, UK) for access to the
573 high- and low-P managed soils. This study was funded by the Novo Nordisk Foundation (Grant
574 number: NNF19SA0059360) and the Biotechnology and Biological Sciences Research
575 Council (BBSRC) as part of the Collaborative Training Program for Sustainable Agricultural
576 Innovation (CTP-SAI) (grant BB/W009439/1) in partnership with The Morley Agricultural

577 Foundation (TMAF). We thank Stephen Rawsthorne (TMAF) and Jonathan Atkinson
578 (University of Nottingham, UK) for their inputs into IT's PhD. Further support to CHH was
579 provided by the European Molecular Biology Organization (EMBO) and the Monogram
580 Network.

581 Competing interests

582 The authors declare no competing interests that may influence the outcome of this work.

583 Author Contributions

584 Courtney Horn Herms: design of the research; performance of the research; data analysis,
585 collection, or interpretation; writing the manuscript. Ian Tsang: data analysis, collection, or
586 interpretation; writing the manuscript. Frederik Bak: data analysis, collection, or
587 interpretation; writing the manuscript. Klara Gunnarsen: data analysis, performance of the
588 research; collection, or interpretation; writing the manuscript. Magdalena Hasenzagl: data
589 analysis, collection, or interpretation; writing the manuscript. Amaru Miranda Djurhuus: data
590 analysis, performance of the research; collection, or interpretation; writing the manuscript.
591 Tom Thirkell: data analysis, collection, or interpretation; writing the manuscript. Eric Ober:
592 design of the research; data analysis, collection, or interpretation; writing the manuscript.
593 Fiona Leigh: design of the research; data analysis, collection, or interpretation; writing the
594 manuscript. James Cockram: design of the research; data analysis, collection, or
595 interpretation; writing the manuscript. Mette Haubjerg Nicolaisen: design of the research;
596 data analysis, collection, or interpretation; writing the manuscript.

597 Data Availability

598 16S rRNA amplicon sequence data is publicly available on NCBI under BioProject
599 PRJNA1308004. Raw data is presented in the figures when applicable. All other raw data is
600 available upon request.

601 References

602 An, R., & Moe, L. A. (2016). Regulation of Pyrroloquinoline Quinone-Dependent Glucose
603 Dehydrogenase Activity in the Model Rhizosphere-Dwelling Bacterium Pseudomonas putida KT2440.
604 *Applied and Environmental Microbiology*, *82*(16), 4955–4964. https://doi.org/10.1128/AEM.00813-
605 16

606 Andersen, K. S., Kirkegaard, R. H., Karst, S. M., & Albertsen, M. (2018). ampvis2: An R package to
607 analyse and visualise 16S rRNA amplicon data. *bioRxiv*. https://doi.org/10.1101/299537

608 Azaroual, S. E., Hazzoumi, Z., Mernissi, N. E., Aasfar, A., Meftah Kadmiri, I., & Bouizgarne, B. (2020).
609 Role of Inorganic Phosphate Solubilizing Bacilli Isolated from Moroccan Phosphate Rock Mine and

Rhizosphere Soils in Wheat (Triticum aestivum L) Phosphorus Uptake. *Current Microbiology*, *77*(9), 2391–2404. https://doi.org/10.1007/s00284-020-02046-8

Bates, T. R., & Lynch, J. P. (1996). Stimulation of root hair elongation in Arabidopsis thaliana by low phosphorus availability. *Plant, Cell & Environment*, *19*(5), 529–538. https://doi.org/10.1111/j.1365-3040.1996.tb00386.x

Benjamini, Y., & Hochberg, Y. (1995). Controlling the False Discovery Rate: A Practical and Powerful Approach to Multiple Testing. *Journal of the Royal Statistical Society: Series B (Methodological)*, *57*(1), 289–300. https://doi.org/10.1111/j.2517-6161.1995.tb02031.x

Bergkemper, F., Schöler, A., Engel, M., Lang, F., Krüger, J., Schloter, M., & Schulz, S. (2016). Phosphorus depletion in forest soils shapes bacterial communities towards phosphorus recycling systems. *Environmental Microbiology*, *18*(6), 1988–2000. https://doi.org/10.1111/1462-2920.13188

Bodenhausen, N., Deslandes-Hérold, G., Waelchli, J., Held, A., van der Heijden, M. G. A., & Schlaeppi, K. (2021). Relative qPCR to quantify colonization of plant roots by arbuscular mycorrhizal fungi. *Mycorrhiza*, *31*(2), 137–148. https://doi.org/10.1007/s00572-020-01014-1

Brown, L. K., George, T. S., Thompson, J. A., Wright, G., Lyon, J., Dupuy, L., Hubbard, S. F., & White, P. J. (2012). What are the implications of variation in root hair length on tolerance to phosphorus deficiency in combination with water stress in barley (Hordeum vulgare)? *Annals of Botany*, *110*(2), 319–328. https://doi.org/10.1093/aob/mcs085

Brundrett, M., Bougher, N., Dell, B., Grove, T., & Malajczuk, N. (1996). *Working with Mycorrhizas in Forestry and Agriculture*. https://doi.org/10.13140/2.1.4880.5444

Buddrus-Schiemann, K., Schmid, M., Schreiner, K., Welzl, G., & Hartmann, A. (2010). Root Colonization by Pseudomonas sp. DSMZ 13134 and Impact on the Indigenous Rhizosphere Bacterial Community of Barley. *Microbial Ecology*, *60*(2), 381–393. https://doi.org/10.1007/s00248-010-9720-8

Callahan, B. J., McMurdie, P. J., Rosen, M. J., Han, A. W., Johnson, A. J. A., & Holmes, S. P. (2016). DADA2: High-resolution sample inference from Illumina amplicon data. *Nature Methods*, *13*(7), 581–583. https://doi.org/10.1038/nmeth.3869

Dai, Z., Liu, G., Chen, H., Chen, C., Wang, J., Ai, S., Wei, D., Li, D., Ma, B., Tang, C., Brookes, P. C., & Xu, J. (2020). Long-term nutrient inputs shift soil microbial functional profiles of phosphorus cycling in diverse agroecosystems. *The ISME Journal*, *14*(3), 757–770. https://doi.org/10.1038/s41396-019-0567-9

De Coster, W., D'Hert, S., Schultz, D. T., Cruts, M., & Van Broeckhoven, C. (2018). NanoPack: Visualizing and processing long-read sequencing data. *Bioinformatics*, *34*(15), 2666–2669. https://doi.org/10.1093/bioinformatics/bty149

Delhaize, E., Rathjen, T. M., & Cavanagh, C. R. (2015). The genetics of rhizosheath size in a multiparent mapping population of wheat. *Journal of Experimental Botany*, *66*(15), 4527–4536. https://doi.org/10.1093/jxb/erv223

Fox, J., & Weisberg, S. (2019). *An R Companion to Applied Regression* (Third). Sage. https://www.john-fox.ca/Companion/

Gahoonia, T. S., Nielsen, N. E., Joshi, P. A., & Jahoor, A. (2001). A root hairless barley mutant for elucidating genetic of root hairs and phosphorus uptake. *Plant and Soil*, *235*(2), 211–219. https://doi.org/10.1023/A:1011993322286

Galloway, A. F., Akhtar, J., Burak, E., Marcus, S. E., Field, K. J., Dodd, I. C., & Knox, P. (2022). Altered properties and structures of root exudate polysaccharides in a root hairless mutant of barley. *Plant Physiology*, *190*(2), 1214–1227. https://doi.org/10.1093/plphys/kiac341

Ge, A.-H., & Wang, E. (2025). Exploring the plant microbiome: A pathway to climate-smart crops. *Cell*, *188*(6), 1469–1485. https://doi.org/10.1016/j.cell.2025.01.035

Guan, Y., Bak, F., Hennessy, R. C., Horn Herms, C., Elberg, C. L., Dresbøll, D. B., Winding, A., Sapkota, R., & Nicolaisen, M. H. (2024). The potential of Pseudomonas fluorescens SBW25 to produce viscosin enhances wheat root colonization and shapes root-associated microbial communities in a plant genotype-dependent manner in soil systems. *mSphere*, *9*(7), e00294-24. https://doi.org/10.1128/msphere.00294-24

Haling, R. E., Brown, L. K., Bengough, A. G., Young, I. M., Hallett, P. D., White, P. J., & George, T. S. (2013). Root hairs improve root penetration, root–soil contact, and phosphorus acquisition in soils of different strength. *Journal of Experimental Botany*, *64*(12), 3711–3721. https://doi.org/10.1093/jxb/ert200

Hao, X., Zhu, Y.-G., Nybroe, O., & Nicolaisen, M. H. (2020). The Composition and Phosphorus Cycling Potential of Bacterial Communities Associated With Hyphae of Penicillium in Soil Are Strongly Affected by Soil Origin. *Frontiers in Microbiology*, *10*. https://doi.org/10.3389/fmicb.2019.02951

Helgason, T., Daniell, T. J., Husband, R., Fitter, A. H., & Young, J. P. W. (1998). Ploughing up the wood-wide web? *Nature*, *394*(6692), 431–431. https://doi.org/10.1038/28764

Herms, C. H., Hennessy, R. C., Bak, F., Dresbøll, D. B., & Nicolaisen, M. H. (2022). Back to our roots: Exploring the role of root morphology as a mediator of beneficial plant–microbe interactions. *Environmental Microbiology*, *00*. https://doi.org/10.1111/1462-2920.15926

Herms, C. H., Hennessy, R. C., Bak, F., Guan, Y., Browne, P. D., Nielsen, T. K., Hansen, L. H., Dresbøll, D. B., & Nicolaisen, M. H. (2025). *Pseudomonas* taxonomic and functional microdiversity in the wheat rhizosphere is cultivar-dependent and links to disease resistance profile and root diameter. *Applied Soil Ecology*, *211*, 106116. https://doi.org/10.1016/j.apsoil.2025.106116

Hewins, C. R., Carrino-Kyker, S. R., & Burke, D. J. (2015). Seasonal variation in mycorrhizal fungi colonizing roots of Allium tricoccum (wild leek) in a mature mixed hardwood forest. *Mycorrhiza*, *25*(6), 469–483. https://doi.org/10.1007/s00572-015-0628-5

Jakobsen, I., Chen, B., Munkvold, L., Lundsgaard, T., & Zhu, Y.-G. (2005). Contrasting phosphate acquisition of mycorrhizal fungi with that of root hairs using the root hairless barley mutant. *Plant, Cell & Environment*, *28*(7), 928–938. https://doi.org/10.1111/j.1365-3040.2005.01345.x

Jansa, J., Erb, A., Oberholzer, H.-R., Šmilauer, P., & Egli, S. (2014). Soil and geography are more important determinants of indigenous arbuscular mycorrhizal communities than management practices in Swiss agricultural soils. *Molecular Ecology*, *23*(8), 2118–2135. https://doi.org/10.1111/mec.12706

Jaspers, E., & Overmann, J. (2004). Ecological Significance of Microdiversity: Identical 16S rRNA Gene Sequences Can Be Found in Bacteria with Highly Divergent Genomes and Ecophysiologies. *Applied*

and Environmental Microbiology, *70*(8), 4831–4839. https://doi.org/10.1128/AEM.70.8.4831-4839.2004

Jensen, C. N. G., Pang, J. K. Y., Gottardi, M., Kračun, S. K., Svendsen, B. A., Nielsen, K. F., Kovács, Á. T., Moelbak, L., Fimognari, L., Husted, S., & Schulz, A. (2024). Bacillus subtilis promotes plant phosphorus (P) acquisition through P solubilization and stimulation of root and root hair growth. *Physiologia Plantarum*, *176*(3), e14338. https://doi.org/10.1111/ppl.14338

Jones, C., Olson-Rutz, K., & Dinkins, C. (2024, March). *Nutrient Uptake Timing by Crops to Assist with Fertilizing Decisions*. Montana State University Extension.

Kay, M., Elkin, L. A., Higgins, J. J., & Wobbrock, J. O. (2021). *ARTool: Aligned Rank Transform for Nonparametric Factorial ANOVAs*. https://doi.org/10.5281/zenodo.594511

Krasileva, K. V., Vasquez-Gross, H. A., Howell, T., Bailey, P., Paraiso, F., Clissold, L., Simmonds, J., Ramirez-Gonzalez, R. H., Wang, X., Borrill, P., Fosker, C., Ayling, S., Phillips, A. L., Uauy, C., & Dubcovsky, J. (2017). Uncovering hidden variation in polyploid wheat. *Proceedings of the National Academy of Sciences*, *114*(6), E913–E921. https://doi.org/10.1073/pnas.1619268114

Kumar, A., Shahbaz, M., Koirala, M., Blagodatskaya, E., Seidel, S. J., Kuzyakov, Y., & Pausch, J. (2019). Root trait plasticity and plant nutrient acquisition in phosphorus limited soil. *Journal of Plant Nutrition and Soil Science*, *182*(6), 945–952. https://doi.org/10.1002/jpln.201900322

Lohse, M., Santangeli, M., Steininger-Mairinger, T., Oburger, E., Reemtsma, T., Lechtenfeld, O. J., & Hann, S. (2023). The effect of root hairs on exudate composition: A comparative non-targeted metabolomics approach. *Analytical and Bioanalytical Chemistry*, *415*(5), 823–840. https://doi.org/10.1007/s00216-022-04475-9

Ma, X., Li, X., & Ludewig, U. (2020). Arbuscular mycorrhizal colonization outcompetes root hairs in maize under low phosphorus availability. *Annals of Botany*, *127*(1), 155. https://doi.org/10.1093/aob/mcaa159

Marrassini, V., Ercoli, L., Piazza, G., & Pellegrino, E. (2024). Plant genotype and inoculation with indigenous arbuscular mycorrhizal (AM) fungi modulate wheat productivity and quality of processed products through changes in the frequency of root AM fungal taxa. *Field Crops Research*, *315*, 109456. https://doi.org/10.1016/j.fcr.2024.109456

Martin, B. D., Witten, D., & Willis, A. D. (2020). Modeling microbial abundances and dysbiosis with beta-binomial regression. *The Annals of Applied Statistics*, *14*(1), 94–115. https://doi.org/10.1214/19-AOAS1283

Martin, M. (2011). Cutadapt removes adapter sequences from high-throughput sequencing reads. *EMBnet.Journal*, *17*(1), Article 1. https://doi.org/10.14806/ej.17.1.200

McMurdie, P. J., & Holmes, S. (2013). phyloseq: An R Package for Reproducible Interactive Analysis and Graphics of Microbiome Census Data. *PLOS ONE*, *8*(4), e61217. https://doi.org/10.1371/journal.pone.0061217

Menezes-Blackburn, D., Giles, C., Darch, T., George, T. S., Blackwell, M., Stutter, M., Shand, C., Lumsdon, D., Cooper, P., Wendler, R., Brown, L., Almeida, D. S., Wearing, C., Zhang, H., & Haygarth, P. M. (2018). Opportunities for mobilizing recalcitrant phosphorus from agricultural soils: A review. *Plant and Soil*, *427*(1), 5–16. https://doi.org/10.1007/s11104-017-3362-2

Mousa, W. K., Shearer, C., Limay-Rios, V., Ettinger, C. L., Eisen, J. A., & Raizada, M. N. (2016). Root-hair endophyte stacking in finger millet creates a physicochemical barrier to trap the fungal pathogen Fusarium graminearum. *Nature Microbiology*, *1*(12), 1–12. https://doi.org/10.1038/nmicrobiol.2016.167

Murphy, J., & Riley, J. P. (1962). A modified single solution method for the determination of phosphate in natural waters. *Analytica Chimica Acta*, *27*, 31–36. https://doi.org/10.1016/S0003-2670(00)88444-5

Nguyen, V. L., & Stangoulis, J. (2019). Variation in root system architecture and morphology of two wheat genotypes is a predictor of their tolerance to phosphorus deficiency. *Acta Physiologiae Plantarum*, *41*(7), 109. https://doi.org/10.1007/s11738-019-2891-0

Ober, E. S., Alahmad, S., Cockram, J., Forestan, C., Hickey, L. T., Kant, J., Maccaferri, M., Marr, E., Milner, M., Pinto, F., Rambla, C., Reynolds, M., Salvi, S., Sciara, G., Snowdon, R. J., Thomelin, P., Tuberosa, R., Uauy, C., Voss-Fels, K. P., … Watt, M. (2021). Wheat root systems as a breeding target for climate resilience. *Theoretical and Applied Genetics*, *134*(6), 1645–1662. https://doi.org/10.1007/s00122-021-03819-w

Qi, P.-F., Johnston, A., Balcerzak, M., Rocheleau, H., Harris, L. J., Long, X.-Y., Wei, Y.-M., Zheng, Y.-L., & Ouellet, T. (2012). Effect of salicylic acid on *Fusarium graminearum*, the major causal agent of fusarium head blight in wheat. *Fungal Biology*, *116*(3), 413–426. https://doi.org/10.1016/j.funbio.2012.01.001

Quast, C., Pruesse, E., Yilmaz, P., Gerken, J., Schweer, T., Yarza, P., Peplies, J., & Glöckner, F. O. (2013). The SILVA ribosomal RNA gene database project: Improved data processing and web-based tools. *Nucleic Acids Research*, *41*(D1), D590–D596. https://doi.org/10.1093/nar/gks1219

Quattrone, A., Lopez-Guerrero, M., Yadav, P., Meier, M. A., Russo, S. E., & Weber, K. A. (2024). Interactions between root hairs and the soil microbial community affect the growth of maize seedlings. *Plant, Cell & Environment*, *47*(2), 611–628. https://doi.org/10.1111/pce.14755

R Core Team. (2023). *R: A Language and Environment for Statistical Computing*. R Foundation for Statistical Computing. https://www.R-project.org/

Raymond, N. S., Gómez-Muñoz, B., van der Bom, F. J. T., Nybroe, O., Jensen, L. S., Müller-Stöver, D. S., Oberson, A., & Richardson, A. E. (2021). Phosphate-solubilising microorganisms for improved crop productivity: A critical assessment. *New Phytologist*, *229*(3), 1268–1277. https://doi.org/10.1111/nph.16924

Rengel, Z., Cakmak, I., & White, P. J. (2022). *Marschner's Mineral Nutrition of Plants*. Academic Press.

Richardson, A. E., Lynch, J. P., Ryan, P. R., Delhaize, E., Smith, F. A., Smith, S. E., Harvey, P. R., Ryan, M. H., Veneklaas, E. J., Lambers, H., Oberson, A., Culvenor, R. A., & Simpson, R. J. (2011). Plant and microbial strategies to improve the phosphorus efficiency of agriculture. *Plant and Soil*, *349*(1), 121–156. https://doi.org/10.1007/s11104-011-0950-4

Robertson-Albertyn, S., Alegria Terrazas, R., Balbirnie, K., Blank, M., Janiak, A., Szarejko, I., Chmielewska, B., Karcz, J., Morris, J., Hedley, P. E., George, T. S., & Bulgarelli, D. (2017). Root Hair Mutations Displace the Barley Rhizosphere Microbiota. *Frontiers in Plant Science*, *8*, 1–15. https://doi.org/10.3389/fpls.2017.01094

Ruijter, J. M., Ramakers, C., Hoogaars, W. M. H., Karlen, Y., Bakker, O., van den Hoff, M. J. B., & Moorman, A. F. M. (2009). Amplification efficiency: Linking baseline and bias in the analysis of quantitative PCR data. *Nucleic Acids Research*, *37*(6), e45. https://doi.org/10.1093/nar/gkp045

Saleem, M., Law, A. D., Sahib, M. R., Pervaiz, Z. H., & Zhang, Q. (2018). Impact of root system architecture on rhizosphere and root microbiome. *Rhizosphere*, *6*(March), 47–51. https://doi.org/10.1016/j.rhisph.2018.02.003

Sasse, J., Martinoia, E., & Northen, T. (2018). Feed Your Friends: Do Plant Exudates Shape the Root Microbiome? *Trends in Plant Science*, *23*(1), 25–41. https://doi.org/10.1016/j.tplants.2017.09.003

Saunders, W. M. H., & Williams, E. G. (1955). Observations on the Determination of Total Organic Phosphorus in Soils. *Journal of Soil Science*, *6*(2), 254–267. https://doi.org/10.1111/j.1365-2389.1955.tb00849.x

Schloss, P. D. (2024). Rarefaction is currently the best approach to control for uneven sequencing effort in amplicon sequence analyses. *mSphere*, *9*(2), e00354-23. https://doi.org/10.1128/msphere.00354-23

Seethepalli, A., Dhakal, K., Griffiths, M., Guo, H., Freschet, G. T., & York, L. M. (2021). RhizoVision Explorer: Open-source software for root image analysis and measurement standardization. *AoB PLANTS*, *13*(6), plab056. https://doi.org/10.1093/aobpla/plab056

Simpson, R. J., Oberson, A., Culvenor, R. A., Ryan, M. H., Veneklaas, E. J., Lambers, H., Lynch, J. P., Ryan, P. R., Delhaize, E., Smith, F. A., Smith, S. E., Harvey, P. R., & Richardson, A. E. (2011). Strategies and agronomic interventions to improve the phosphorus-use efficiency of farming systems. *Plant and Soil*, *349*(1), 89–120. https://doi.org/10.1007/s11104-011-0880-1

Smith, S. E., & Smith, F. A. (2011). Roles of arbuscular mycorrhizas in plant nutrition and growth: New paradigms from cellular to ecosystem scales. *Annual Review of Plant Biology*, *62*, 227–250. https://doi.org/10.1146/annurev-arplant-042110-103846

Suzuki, N., Taketa, S., & Ichii, M. (2003). Morphological and physiological characteristics of a root-hairless mutant in rice (Oryza sativa L.). *Plant and Soil*, *255*(1), 9–17. https://doi.org/10.1023/A:1026180318923

Thijs, S., Op De Beeck, M., Beckers, B., Truyens, S., Stevens, V., Van Hamme, J. D., Weyens, N., & Vangronsveld, J. (2017). Comparative Evaluation of Four Bacteria-Specific Primer Pairs for 16S rRNA Gene Surveys. *Frontiers in Microbiology*, *8*. https://doi.org/10.3389/fmicb.2017.00494

Thirkell, T. J., Grimmer, M., James, L., Pastok, D., Allary, T., Elliott, A., Paveley, N., Daniell, T., & Field, K. J. (2022). Variation in mycorrhizal growth response among a spring wheat mapping population shows potential to breed for symbiotic benefit. *Food and Energy Security*, *11*(2), e370. https://doi.org/10.1002/fes3.370

Thirkell, T. J., Pastok, D., & Field, K. J. (2020). Carbon for nutrient exchange between arbuscular mycorrhizal fungi and wheat varies according to cultivar and changes in atmospheric carbon dioxide concentration. *Global Change Biology*, *26*(3), 1725–1738. https://doi.org/10.1111/gcb.14851

Tsang, I., Atkinson, J. A., Rawsthorne, S., Cockram, J., & Leigh, F. (2024). Root hairs: An underexplored target for sustainable cereal crop production. *Journal of Experimental Botany*, erae275. https://doi.org/10.1093/jxb/erae275

Tsang, I., Thomelin, P., Ober, E. S., Rawsthorne, S., Atkinson, J. A., Wells, D. M., Percival-Alwyn, L., Leigh, F. J., & Cockram, J. (2024). A novel root hair mutant, srh1, affects root hair elongation and reactive oxygen species levels in wheat. *Frontiers in Plant Science*, *15*. https://doi.org/10.3389/fpls.2024.1490502

Ulén, B., Bechmann, M., Fölster, J., Jarvie, H. P., & Tunney, H. (2007). Agriculture as a phosphorus source for eutrophication in the north-west European countries, Norway, Sweden, United Kingdom and Ireland: A review. *Soil Use and Management*, *23*(s1), 5–15. https://doi.org/10.1111/j.1475-2743.2007.00115.x

Van Kauwenbergh, S. (2010). *World Phosphate Rock Reserves and Resources*. IFDC Publications. https://pdf.usaid.gov/pdf_docs/Pnadw835.PDF

Wang, L., Zhou, J., George, T. S., & Feng, G. (2025). Trade-offs between arbuscular mycorrhizal symbiosis and root hairs in phosphorus source utilization are determined by functional divergence of the rhizosphere bacterial microbiome in barley. *Soil Biology and Biochemistry*, *209*, 109887. https://doi.org/10.1016/j.soilbio.2025.109887

Werner, G. D. A., & Kiers, E. T. (2015). Order of arrival structures arbuscular mycorrhizal colonization of plants. *New Phytologist*, *205*(4), 1515–1524. https://doi.org/10.1111/nph.13092

Wickham, H. (2016). *ggplot2: Elegant Graphics for Data Analysis*. Springer-Verlag New York. https://ggplot2.tidyverse.org

Xiao, J., Dong, S., Shen, H., Li, S., Wessell, K., Liu, S., Li, W., Zhi, Y., Mu, Z., & Li, H. (2022). N Addition Overwhelmed the Effects of P Addition on the Soil C, N, and P Cycling Genes in Alpine Meadow of the Qinghai-Tibetan Plateau. *Frontiers in Plant Science*, *13*. https://doi.org/10.3389/fpls.2022.860590

Yi, H., Hu, S., Zhang, Y., Wang, X., Xia, Z., Lei, Y., & Duan, M. (2023). Proper Delay of Phosphorus Application Promotes Wheat Growth and Nutrient Uptake under Low Phosphorus Condition. *Agriculture*, *13*(4), Article 4. https://doi.org/10.3390/agriculture13040884

Zadoks, J. C., Chang, T. T., & Konzak, C. F. (1974). A decimal code for the growth stages of cereals. *Weed Research*, *14*(6), 415–421. https://doi.org/10.1111/j.1365-3180.1974.tb01084.x

Zhang, C., Simpson, R. J., Kim, C. M., Warthmann, N., Delhaize, E., Dolan, L., Byrne, M. E., Wu, Y., & Ryan, P. R. (2018). Do longer root hairs improve phosphorus uptake? Testing the hypothesis with transgenic Brachypodium distachyon lines overexpressing endogenous genes. *New Phytologist*, *217*(4), 1654–1666. https://doi.org/10.1111/nph.14980

Zhou, J., Zhang, L., Feng, G., & George, T. S. (2022). Arbuscular mycorrhizal fungi have a greater role than root hairs of maize for priming the rhizosphere microbial community and enhancing rhizosphere organic P mineralization. *Soil Biology and Biochemistry*, *171*, 108713. https://doi.org/10.1016/j.soilbio.2022.108713

Zhu, R., Chen, C., Chen, M., Miroslav, V., Dao, J., Xing, Y., Kong, D., Chen, B., & Wang, Z. (2025). How Arbuscular Mycorrhizal Fungi Shape Plant Root Morphology: A Global Meta-Analysis. *Plant, Cell & Environment*. https://doi.org/10.1111/pce.70082